

Degradation of Toxic Indigo Carmine Dye by Electrosynthesized Ferrate (VI)

S. Barisci*, H. Inan, O. Turkay, A. Dimoglo and D. Erol

Gebze Technical University, Environmental Engineering Department, 41400, Gebze, Kocaeli, Turkey

Abstract: Response surface methodology was applied for optimizing indigo carmine (IC) dye removal by electrochemically produced ferrate (VI). Box-Behnken design was employed in this study, and design parameters were pH, Fe (VI) dose and initial dye concentration (C_0). R^2 and adjusted R^2 values were very high that indicated very good accuracy for the employed model. Optimum operational conditions were: 4.08-7.69 for pH, 24-118.83 mg/L for Fe (VI) dose and 60.68-99.13 mg/L for complete removal of IC. Produced by electrochemical method Ferrate (VI) provides high effectiveness for IC dye-containing synthetic wastewater.

Keywords: Box-Behnken design, Ferrate (VI), Indigo carmine, Response surface methodology.

1. INTRODUCTION

Textile industries consume large amount of fresh water during its unit processes and the water is contaminated by toxic chemicals. Especially, dyeing process during manufacturing facilities has the biggest risk to the environment due to high concentrations [1]. Discharging this type of wastewater directly into the surface waters causes negative effects on the flora and fauna.

Dyes have been commonly used in textile, paper and pulp, dyeing, tannery, printing, photographic, and coating industries. Frequently, the dye wastewaters cover dye pigments, non-biodegradable organic and inorganic substances. When dye wastewaters are discharged to the aquatic bodies, they hinder the biological processes such as photosynthesis, blocking light penetration in the water of lakes and rivers [2].

Indigo carmine (IC) is a fairly toxic dye which is used primarily in the production of denim textile. The contact with indigo may cause some irritations on skin and eye. Also it can cause harm to cornea and conjunctiva. It is known that IC dye is cancer-causing chemical and can cause acute toxicity. It has also been proved that the dye causes tumour when it is consumed [3]. For those reasons, release of IC without any treatment into the aquatic bodies is harmful and causes such diseases. However, since IC has symmetrical structure and strong stability, it is difficult to be degraded. Thus, recent researches take cognizance of the removal of IC dye-containing wastewaters. The technologies used for the

degradation of IC and other dyes consist of adsorption [4-8], aerobic bioreactors [9] and advanced oxidation processes such as electrooxidation [10-12], photocatalysis [13-21] and electrocoagulation [2, 22]. Although those methods seem to be efficient technologies, physical adsorption and coagulation transfer the contaminants from wastewater to other environment which resulted sludge production and advanced oxidation processes are expensive technologies. Additionally, dye wastewater requires treatment with new techniques due to its high concentration of organic compounds and toxicity. Ferrate (VI) is capable of decomposing many toxic dyes to low-toxic products, and also of disinfecting wastewater. Its application is effective even by very low (0.005–0.04 mg/L) doses of ferrate (VI). Unlike dry salts, the ferrate (VI) solution is not stable. Ferrate (VI) is expensive chemical, when a multi-stage synthesis is used to obtain them. All these disadvantages can be overcome when preparing ferrate (VI) by electrochemical method [23-25]. So that electrosynthesized ferrate (VI) is a promising technology for the treatment of water and wastewater due to its high oxidizing power and coagulant effect. These properties make ferrate (VI) very effective during the degradation processes. Ferrate (VI) can provide high degradation efficiency or it provides complete mineralization of contaminants without producing toxic by-products [26-32].

Response surface methodology (RSM) is a group of mathematical and statistical methods used for the optimization of output variables which are affected by many input factors [33]. It can be also used for the evaluation of interaction between individual variables. Recent studies have shown that RSM could be useful for the optimization of factors influenced on the processes [34-36]. RSM has been applied effectively

*Correspondence Address to this author at the Gebze Technical University, Environmental Engineering Department, 41400, Gebze, Kocaeli, Turkey; Tel: +902626053208; Fax: +902626053145; E-mail: sbarisci@gtu.edu.tr

for the removal of many pollutants by advanced oxidation processes [37-40].

In this study, degradation of highly toxic IC dye by electrochemically produced ferrate (VI) ion was investigated. RSM was used for optimization of the process according to color and chemical oxygen demand (COD) removal efficiencies relative to the key parameters, such as initial dye concentration, pH and ferrate (VI) dose.

2. MATERIALS AND METHODS

2.1. Chemicals

IC (dye content 95%) and sodium hydroxide (anhydrous pellets and with 98% purity) were supplied from Sigma-Aldrich. Buffers were used to adjust pH values: $C_8H_5KO_4$ -HCl solution (pH 4); KH_2PO_4 -NaOH solution (pH 7); $Na_2B_4O_7 \cdot 10H_2O$ -NaOH solution (pH 10). Indigo dye containing synthetic wastewater was prepared as follows: 150 mg IC dye was added to 1% NaOH solution and 5% sodium thiosulfate solution mixture and completed to 1000 ml. Initial COD value of the prepared solution was 320 mg/L and initial color value was 130 pt-co.

2.2. Electrolytic System and Experimental Procedures

In our study, ferrate (VI) synthesis was conducted in an electrolysis cell made of plexiglass material with the dimensions of 12x7x5 cm. Electrodes were high purity iron plates with the dimensions of 10x5x0.2 cm. Active electrode surface area was 156 cm². NaOH was used to provide highly alkaline media. Current was supplied by DC power source. Details for optimal conditions of ferrate (VI) synthesis and its stability report can be found in our previous study [41]. All experiments were conducted using Box-Behnken experimental design: different ferrate (VI) doses (24, 72 and 100 mg/L as Fe (VI)), initial dye concentrations (20, 60 and 120 mg/L) and pH values (4, 7 and 10). After synthesis of ferrate (VI), desired amount of ferrate (VI) was dosed to indigo containing solution, and then pH was adjusted to the mentioned values with the buffer solutions: $C_8H_5KO_4$ -HCl solution (pH 4); KH_2PO_4 -NaOH solution (pH 7); $Na_2B_4O_7 \cdot 10H_2O$ -NaOH solution (pH 9). The initial pH of the IC solution was 11.5 ± 0.2. Rapid and slow mixing was applied for 30 seconds and 20 minutes, respectively. After mixing procedure, sedimentation took place for one hour in the process. The supernatant was taken from the treated solution and all samples were filtered through 0.45 μm membrane

filters for the COD and color measurements. All experiments were performed at the room temperature.

2.3. Analytical Methods

COD was determined according to Standard Methods. Color was measured via HACH Lange DR 2800 spectrophotometer. Ferrate (VI) concentration was measured by HACH Lange DR 5000 UV-VIS spectrophotometer at a pre-determined wave length of 505 nm.

2.4. Mathematical and Statistical Procedures

In this study, the design of experiments was prepared using Box-Behnken model and three input factors were selected (A: pH, B: Fe (VI) dose, C: initial dye concentration) for the optimization of indigo dye degradation by ferrate (VI) ion according to the two different responses (R_1 , color removal and R_2 , COD removal).

The removal efficiencies were fitted to a general function indicating the interaction between dependent and independent variables using second-order polynomial equation. The employed model of the second order polynomial is:

$$R = \beta_0 + \sum \beta_i X_i + \sum \beta_{ii} X_i^2 + \sum \beta_{ij} X_i X_j \quad (1)$$

Where R is the response which is predicted by the model, X_i and X_j are independent input factors, β_0 is the intercept, β_i is a linear coefficient, β_{ii} is a quadratic coefficient and β_{ij} is the interaction coefficient.

To determine the influence of selected parameters on the process efficiency for indigo dye removal, different levels were chosen for each parameter. The selection of operating levels is summarized in Table S1.

Design expert, version 8.0.4.1 (STAT-EASE Inc., Minneapolis, USA) was used for the preparation of experimental design and the analysis of obtained data. The analysis of variance (ANOVA) was run for prediction of the statistical parameters.

3. RESULTS AND DISCUSSION

3.1. Design of Experiments and ANOVA Report

Table 1 shows the summary of experimental planning and each response from the point of the efficiencies on color and COD removal.

Table 1: Experimental Plan for Box-Behnken Design and Responses in each Experiment

Run	Real pH	Real Fe(VI) dose (mg/L)	Real C _o (mg/L)	R ₁ , Colour removal (%)	R ₂ , COD removal (%)
1	7	72	60	98.95	80
2	7	120	100	99.09	92.3
3	4	72	100	97.59	85.7
4	7	72	60	99.73	80.95
5	10	120	60	92.5	51.26
6	4	120	60	97.9	85.71
7	7	72	60	98.68	85.39
8	4	24	60	98.42	72.63
9	7	72	60	99.21	84.28
10	10	72	100	93.54	67.19
11	7	24	100	98.79	80.43
12	7	120	20	91.37	33
13	4	72	20	87.06	50.6
14	10	72	20	99.13	33.47
15	7	24	20	99.13	81.7
16	10	24	60	99.9	85.07
17	7	72	60	98.95	87.3

The ANOVA analysis indicates the significance of each parameter and also significance of the interaction between variables. ANOVA results can be seen in Table 2.

Probability value (Prob>F), F-value (Fisher variation ratio) of the model and adequate precision are the main points presenting the significance and acceptability of the model employed in the study. According to the

Table 2: ANOVA Results for Response Surface Quadratic Model

R ₁ , Color removal				R ₂ , COD removal			
Factor	Sum of squares	F-ratio	p-value (Prob>F)	Factor	Sum of squares	F-ratio	p-value (Prob>F)
Model	194.44	7.87	0.0063 (significant)	Model	5631.78	40.74	<0.0001 (significant)
A: pH	2.10	0.77	0.4107	A: pH	415.44	27.05	0.0013
B: Fe (VI) dose	29.57	10.77	0.0135	B: Fe (VI) dose	414.14	26.96	0.0013
C: C _o	18.97	6.91	0.0340	C: C _o	2011.37	130.96	<0.0001
AB	11.83	4.31	0.0765	AB	549.67	35.79	0.0006
AC	64.96	23.66	0.0018	AC	0.48	0.031	0.8652
BC	16.24	5.91	0.0453	BC	917.18	59.72	0.0001
A ²	23.14	8.43	0.0229	A ²	534.51	34.80	0.0006
B ²	0.74	0.27	0.6186	B ²	7.68	0.50	0.5024
C ²	24.85	9.05	0.0197	C ²	720.03	46.88	0.0002
Residual	19.22			Residual	107.51		
Lack of fit	18.59	39.33	0.0020 (significant)	Lack of fit	70.18	2.51	0.1980 (not significant)
Pure Error	0.63			Pure Error	37.34		
Cor Total	213.67			Cor Total	5739.30		

Table 3: ANOVA Results of the Polynomial Regression Model Established for Oxidation of Indigo Dye by Electrosynthesized Fe (VI)

Parameter	R ₁ , Colour removal (%)	R ₂ , COD removal (%)
R ²	0.91	0.9813
Adjusted R ²	0.7944	0.9572
Prob > F	0.0063	<0.0001
Model F value	7.87	40.74
Std. Deviation	1.66	3.92
PRESS	298.44	1181.16
Adequate precision	10.298	20.626

ANOVA report, the model F-values of 7.87 and 40.74 imply the model's significance, and values of "Prob > F" less than 0.0500 specify that the terms of the model are significant. In our case; B, C, AC, BC, A² and C² for color removal and A, B, C, AB, BC, A², and C² for COD removal are significant terms of the model (see Table 2).

The correlation factors R² are equal to 0.9813 and 0.91 for COD and color removal, as seen in Table 3. Model parameters for two responses (color and COD removal) are summarized, as well (see Table 2). High R² values state that the total variation could be depicted by the model established in the present study phrasing a sufficient quadratic fit.

When second order polynomial model is considered (eq. 1), following expressions were obtained according to RSM:

$$\text{Color removal (\%)} = 99.28 - 1.92xB + 1.54xC - 4.03xAxC + 2.01xBxC - 2.32xA^2 - 2.41xC^2 \quad (2)$$

$$\text{COD removal (\%)} = 78.37 - 7.21xA - 7.20xB + 15.86xC - 11.72xAxB + 15.14xBxC - 11.27xA^2 \quad (3)$$

Where A is pH, B is Fe (VI) dose and C shows initial dye concentration.

3.2. Graphical Elucidation of the Model

3.2.1. Color Removal Efficiency

Experimental results fitted the employed model with high R² value and were close to predicted values. They indicate that R² and adjusted R² values for the model is satisfactory (see Figure S1 in supplementary materials).

Figure 1 demonstrates the effect of different factors on the process in terms of color removal efficiency. As

seen in Figure 1, color removal efficiency increased after pH value (A) had become closer to the reference point (0). Then the efficiency decreased, while the pH value became distant from the reference point. This situation indicates that the efficiency increases from acidic values through neutral values of pH, and then color removal efficiency decreases with increasing pH. The range of applied Fe (VI) doses (B) supplied efficient removal in color, as the efficiency was above 95% for all doses. The change of Fe (VI) dose between selected ranges seemed not providing accurate difference on color removal.

The effect of initial dye concentration (C) can be seen in Figure 1. According to Figure 1, color removal efficiency increased with increase of initial dye concentration until the reference point, and there was slight increase after reference point, too. But further increase of initial dye concentration until the maximum point (+1) caused decrease in color removal efficiency. This means, that the efficiency increases with increasing dye concentration until certain point, only.

Figure 2 shows 3D graphics of the model. The effect of Fe (VI) dose on color removal efficiency at a constant initial dye concentration of 60 mg/L for different pH values was predicted. Color removal efficiency showed an increment with regard to increasing pH up to neutral values, and then the efficiency displayed decreasing trend in alkaline values. Fe (VI) dose role in color removal was insignificant, as far as high color removal efficiencies (>95%) were obtained in all applied Fe (VI) doses, as seen in Figure 2a.

Figure 2b illustrates the interaction between color removal efficiency and initial dye concentration for different pH conditions at constant Fe (VI) dose (72 mg/L). The presence of higher dye concentrations,

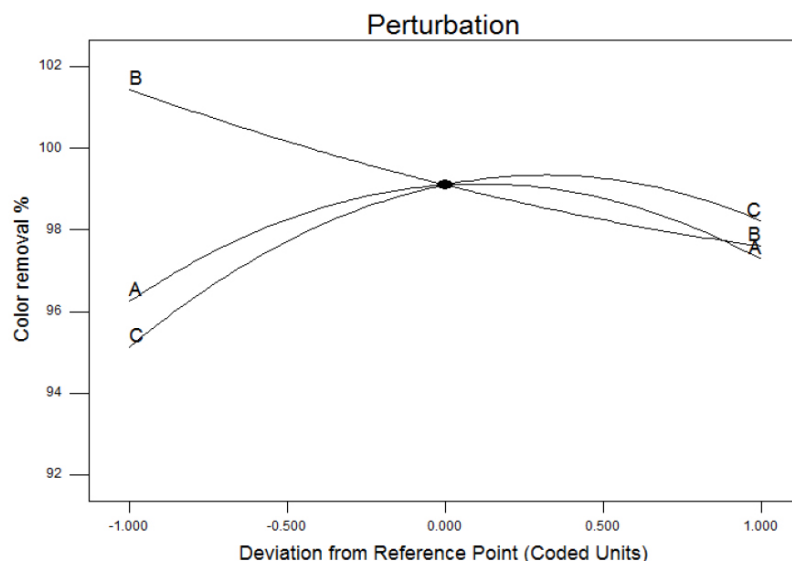


Figure 1: Perturbation plot for colour removal.

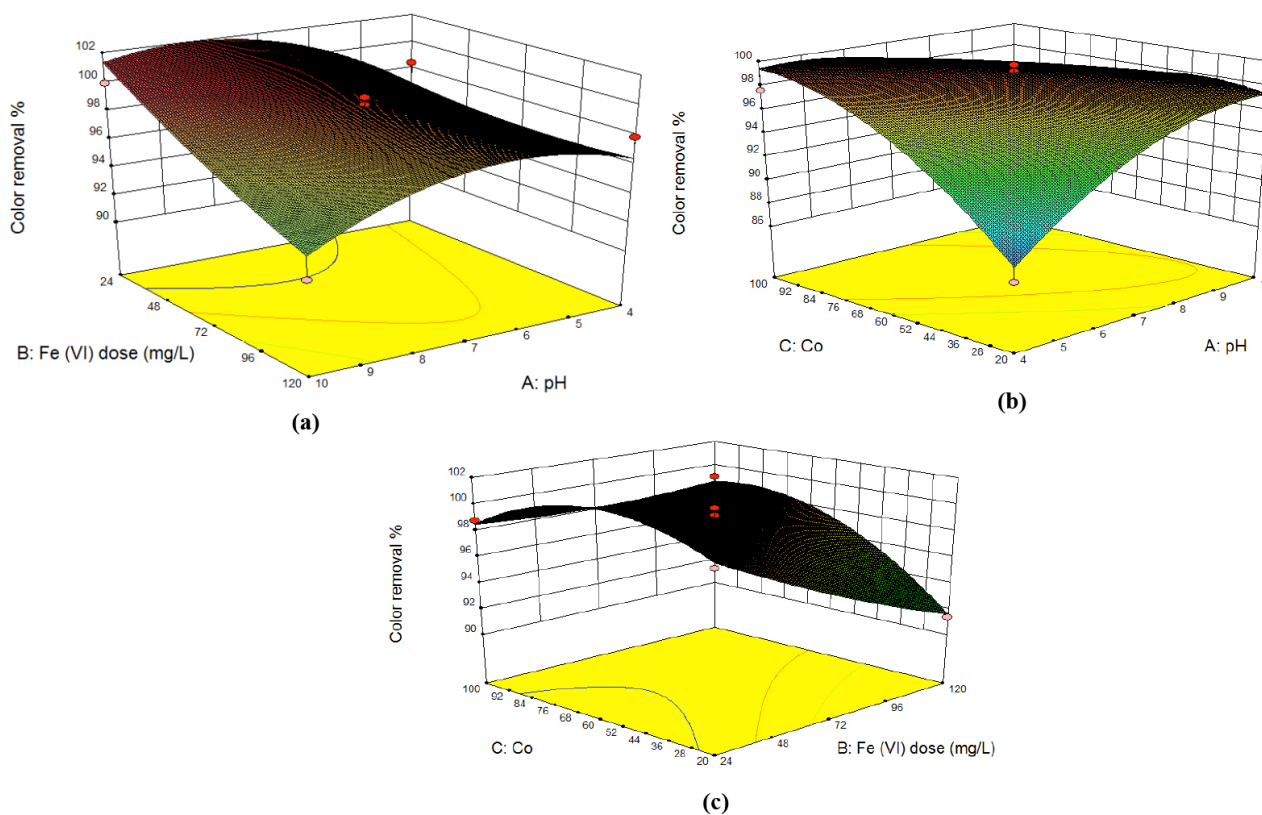


Figure 2: 3D surface plot for colour removal as a function of (a) Fe (VI) dose and pH; (b) initial dye concentration and pH and (c) initial dye concentration and pH.

together with neutral and alkaline conditions, was found to be more desirable for the indigo dye removal.

Figure 2c shows the interaction between initial dye concentration and Fe (VI) dose at pH 7. Lower Fe (VI) doses and higher dye concentrations showed higher color removal efficiency (>98%).

3.2.2. COD Removal Efficiency

According to Figure 3, COD removal efficiency did not change by the variation of Fe (VI) dose as much as pH and initial dye concentration. The same behaviour with color removal was observed on COD removal. When pH value (A) became closer to reference point,

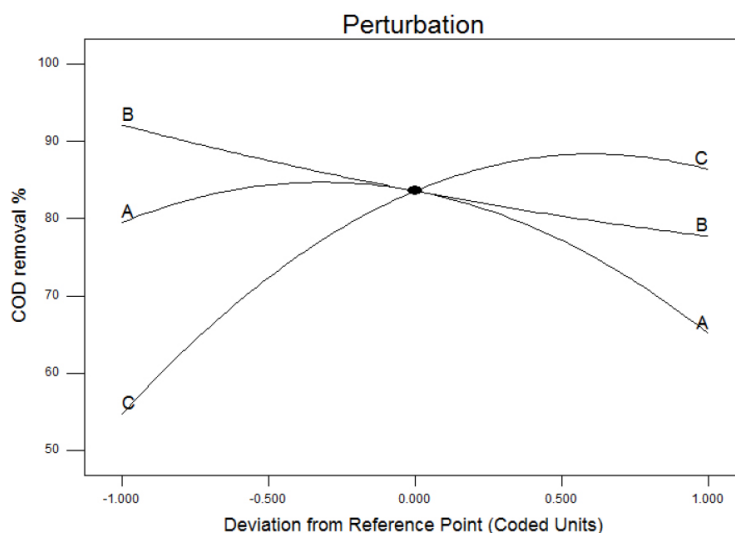


Figure 3: Perturbation plot for COD removal.

COD removal increased, but the efficiency started to decrease, when pH value became distant from reference point (0). Initial dye concentration affected COD removal more than color removal, as the change of efficiency was between 55-85%. However, the trend was almost the same with color removal. While initial dye concentration was getting closer to the reference

point, the efficiency was increasing. In contrast to color removal (Figure 1), the efficiency continued to increase after reference point for a while and then decreased until the maximum point.

As it can be shown in Figure 4a, the response was plain surface, which implies that there is no such

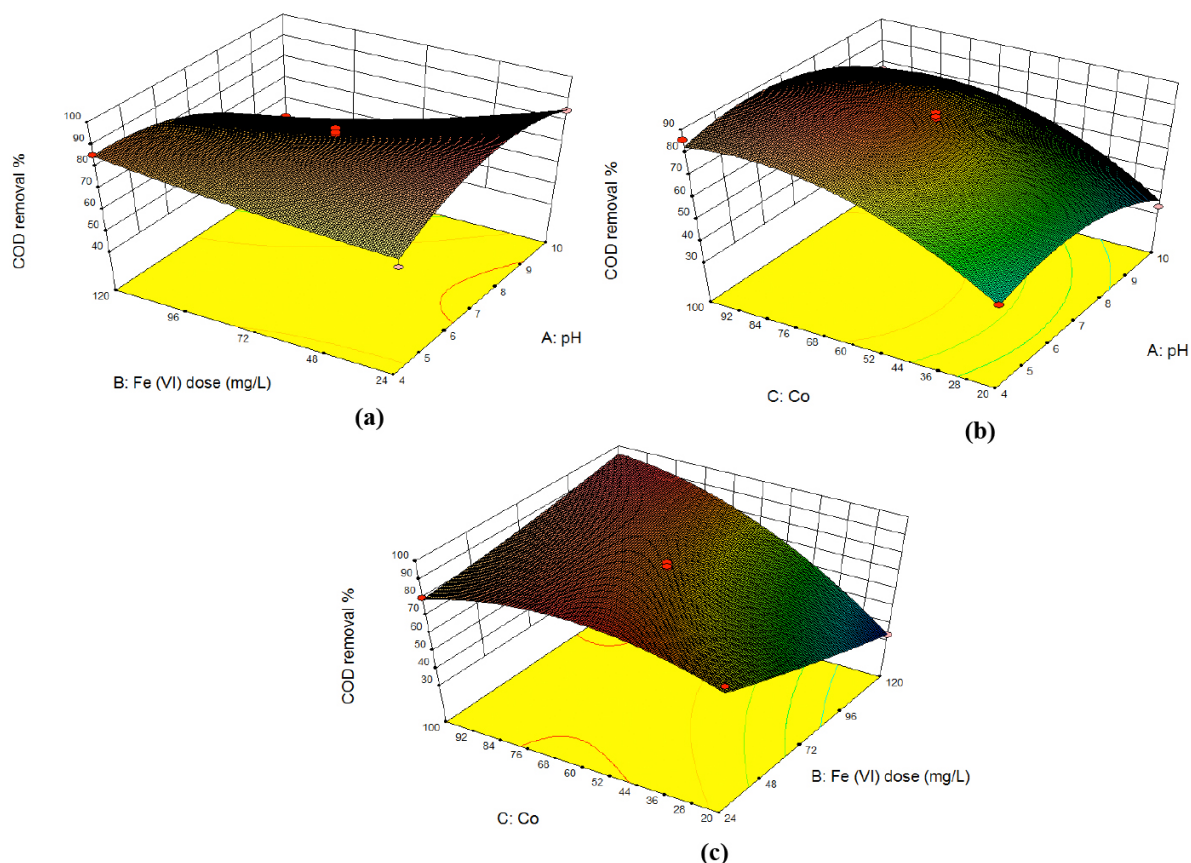


Figure 4: 3D surface plot for COD removal as a function of (a) Fe (VI) dose and pH; (b) initial dye concentration and pH and (c) initial dye concentration and pH.

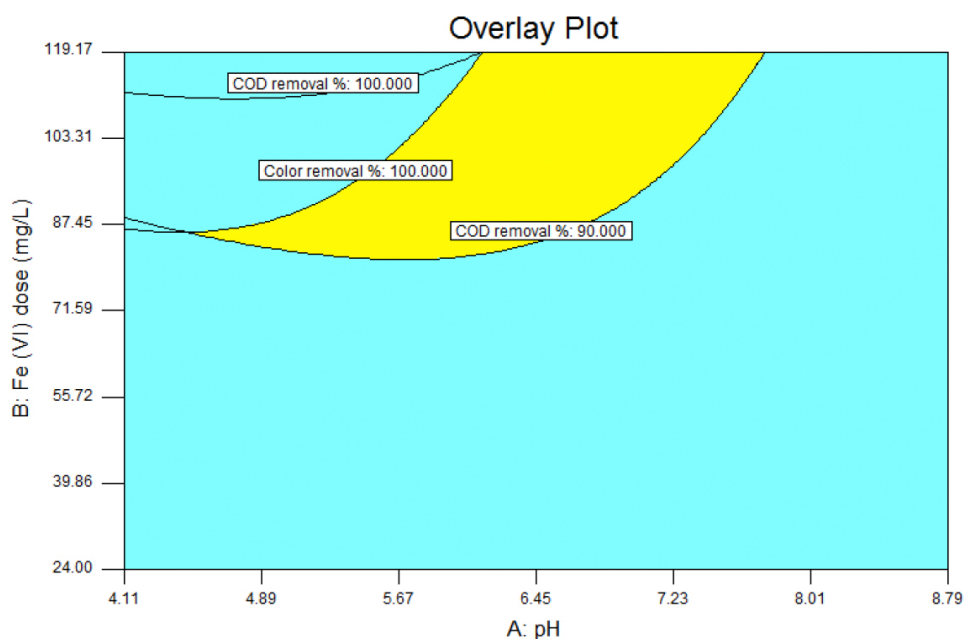


Figure 5: Overlay plot for the optimal region.

interaction between these variables (Fe (VI) dose and pH) on the removal of COD. The change of pH had a dominant effect, compared to Fe (VI) dose, on the removal efficiency, as the slope was due to pH change, while Fe (VI) dose affected the process slightly.

In Figure 4b, 3D graphic of the model was convex surface, and maximum COD removal efficiency was obtained in the final region of initial dye concentration for the studied values. Through the neutral pH values, the removal efficiency increased, and after the neutral values there was a decrease through the final region of studied pH values.

Figure 4c shows that there was an interaction between Fe (VI) dose and initial dye concentration. COD removal efficiency was decreased, while Fe (VI) dose increased. Also, middle value of initial concentration showed high efficiency on COD removal.

3.4. Optimization Step

According to the Design Expert version 8.0.4.1 software, the desired goal for each condition (pH, Fe (VI) dose and initial dye concentration) was chosen as "in range". The programme found 27 solutions, which help to achieve optimum conditions for color and COD removal with high desirability range of 0.943-1. The maximum predicted color and COD removal was 102% and 100%, respectively. The ranges of optimum operational conditions for each parameter were: 4.08-7.69 for pH, 24-119.17 mg/L for Fe (VI) dose and 60.68-99.13 mg/L for initial dye concentration. On the

other part, the desirability function approach was used to maximize both color and COD removal. Initial dye concentration was fixed to the middle value (60 mg/L) to achieve such a goal. The overlay plot for the optimal region is shown in Figure 5. The yellow portion gave the allowable values of the two variables (Fe (VI) dose and pH) by maximizing removal efficiencies of color and COD. According to Figure 5, if the process was conducted at pH range of 4.52-7.69 and Fe (VI) dose range of 79.55-119.17 mg/L, both color and COD removal would be maximized for initial dye concentration of 60 mg/L. Also, the calculated values for the validation experiments were found to be satisfactory (see Table S2 in supplementary material).

CONCLUSIONS

Response surface methodology (RSM) is a simple way for the optimization of the parameters for dye removal from textile waste water. RSM reduces the number of experiments. Besides, RSM provides important information about interactions between operational parameters. In this study, the model employed provided high accuracy with high R^2 values (0.91 for color removal and 0.9813 for COD removal). Electrochemically produced ferrate (VI) was very effective for IC dye removal in terms of color and COD removal.

ACKNOWLEDGEMENT

This study was supported by Gebze Technical University in the frameworks of the project no: 2013-A21.

SUPPLEMENTARY MATERIALS

The supplementary materials can be downloaded from the journal website along with the article.

REFERENCES

- [1] Van der Bruggen B, Curcio E, Drioli E. Process intensification in the textile industry: the role of membrane technology. *J Environ Manage* 2004; 73(3): 267-74. <https://doi.org/10.1016/j.jenvman.2004.07.007>
- [2] Secula MS, Crețescu I, Petrescu S. An experimental study of indigo carmine removal from aqueous solution by electrocoagulation. *Desalination* 2011; 277(1): 227-35. <https://doi.org/10.1016/j.desal.2011.04.031>
- [3] Jenkins CL. Textile dyes are potential hazards. *J Environ Health* 1978; 40(5): 256-63.
- [4] Prado AG, Torres JD, Faria EA, Dias SIC. Comparative adsorption studies of indigo carmine dye on chitin and chitosan. *J Colloid Interface Sci* 2004; 277(1): 43-7. <https://doi.org/10.1016/j.jcis.2004.04.056>
- [5] Mittal A, Kurup L, Mittal J. Freundlich and Langmuir adsorption isotherms and kinetics for the removal of Tartrazine from aqueous solutions using hen feathers. *J Hazard Mater* 2007; 146(1): 243-8. <https://doi.org/10.1016/j.jhazmat.2006.12.012>
- [6] Cestari AR, Vieira EF, Tavares AM, Bruns RE. The removal of the indigo carmine dye from aqueous solutions using cross-linked chitosan—Evaluation of adsorption thermodynamics using a full factorial design. *J Hazard Mater* 2008; 153(1): 566-74. <https://doi.org/10.1016/j.jhazmat.2007.08.092>
- [7] Lakshmi UR, Srivastava VC, Mall ID, Lataye DH. Rice husk ash as an effective adsorbent: evaluation of adsorptive characteristics for Indigo Carmine dye. *J Environ Manage* 2009; 90(2): 710-20. <https://doi.org/10.1016/j.jenvman.2008.01.002>
- [8] Kesraoui A, Selmi T, Seffen M, Brouers F. Influence of alternating current on the adsorption of indigo carmine. *Environ Sci Pollut Res* 2016; 1-11.
- [9] Khelifi E, Gannoun H, Touhami Y, Bouallagui H, Hamdi M. Aerobic decolorization of the indigo dye-containing textile wastewater using continuous combined bioreactors. *J Hazard Mater* 2008; 152(2): 683-9. <https://doi.org/10.1016/j.jhazmat.2007.07.059>
- [10] Sanroman M, Pazos M, Ricart M, Cameselle C. Decolourisation of textile indigo dye by DC electric current. *Eng Geo* 2005; 77(3): 253-61. <https://doi.org/10.1016/j.enggeo.2004.07.016>
- [11] Butrón E, Juárez ME, Solis M, Teutli M, González I, Nava JL. Electrochemical incineration of indigo textile dye in filter-press-type FM01-LC electrochemical cell using BDD electrodes. *Electrochim Acta* 2007; 52(24): 6888-94. <https://doi.org/10.1016/j.electacta.2007.04.108>
- [12] Palma-Goyes RE, Silva-Agredo J, González I, Torres-Palma RA. Comparative degradation of indigo carmine by electrochemical oxidation and advanced oxidation processes. *Electrochim Acta* 2014; 140: 427-33. <https://doi.org/10.1016/j.electacta.2014.06.096>
- [13] Subramani A, Byrappa K, Ananda S, Rai KL, Ranganathaiah C, Yoshimura M. Photocatalytic degradation of indigo carmine dye using TiO₂ impregnated activated carbon. *Bull Mater Sci* 2007; 30(1): 37-41. <https://doi.org/10.1007/s12034-007-0007-8>
- [14] Barka N, Assabane A, Nounah A, Ichou YA. Photocatalytic degradation of indigo carmine in aqueous solution by TiO₂ coated non-woven fibres. *J Hazard Mater* 2008; 152(3): 1054-9. <https://doi.org/10.1016/j.jhazmat.2007.07.080>
- [15] Torrades F, Saiz S, García-Hortal JA. Using central composite experimental design to optimize the degradation of black liquor by Fenton reagent. *Desalination* 2011; 268(1): 97-102. <https://doi.org/10.1016/j.desal.2010.10.003>
- [16] Khataee AR, Zarei M, Moradkhannejhad L. Application of response surface methodology for optimization of azo dye removal by oxalate catalyzed photoelectro-Fenton process using carbon nanotube-PTFE cathode. *Desalination* 2010; 258(1): 112-9. <https://doi.org/10.1016/j.desal.2010.03.028>
- [17] Khataee A, Zarei M, Fathinia M, Jafari MK. Photocatalytic degradation of an anthraquinone dye on immobilized TiO₂ nanoparticles in a rectangular reactor: Destruction pathway and response surface approach. *Desalination* 2011; 268(1): 126-33. <https://doi.org/10.1016/j.desal.2010.10.008>
- [18] Gómez-Solís C, Juárez-Ramírez I, Moctezuma E, Torres-Martínez LM. Photodegradation of indigo carmine and methylene blue dyes in aqueous solution by SiC-TiO₂ catalysts prepared by sol-gel. *J Hazard Mater* 2012; 217: 194-9. <https://doi.org/10.1016/j.jhazmat.2012.03.019>
- [19] Sood S, Kumar S, Umar A, Kaur A, Mehta SK, Kansal SK. TiO₂ quantum dots for the photocatalytic degradation of indigo carmine dye. *J Alloys Compd* 2015; 650: 193-8. <https://doi.org/10.1016/j.jallcom.2015.07.164>
- [20] Yao Y, Cui L, Li Y, Yu N, Dong H, Chen X, et al. Electrochemical Degradation of Methyl Orange on PbO₂-TiO₂ Nanocomposite Electrodes. *Int J Environ Res* 2015; 9(4): 1357-64.
- [21] Naciri N, Farahi A, Rafqah S, Nasrellah H, El Mhammedi MA, Lançar I, et al. Effective photocatalytic decolorization of indigo carmine dye in Moroccan natural phosphate-TiO₂ aqueous suspensions. *Opt Mater* 2016; 52: 38-43. <https://doi.org/10.1016/j.optmat.2015.12.011>
- [22] Tünay O, Şimşeker M, Kabdaşlı I, Ölmez-Hancı T. Abatement of reduced sulphur compounds, colour, and organic matter from indigo dyeing effluents by electrocoagulation. *Environ Technol* 2014; 35(13): 1577-88. <https://doi.org/10.1080/09593330.2013.873824>
- [23] Barişçi S, Turkay O, Dimoglo A. Review on Greywater Treatment and Dye Removal from Aqueous Solution by Ferrate (VI). Ferrites and Ferrates: Chemistry and Applications in Sustainable Energy and Environmental Remediation: ACS Publications 2016; pp. 349-409.
- [24] Sun X, Zhang Q, Liang H, Ying L, Xiangxu M, Sharma VK. Ferrate (VI) as a greener oxidant: Electrochemical generation and treatment of phenol. *J Hazard Mater* 2016; 319: 130-6. <https://doi.org/10.1016/j.jhazmat.2015.12.020>
- [25] Nam J-H, Kim I-K, Kwon J, Kim YD. Applications of electrochemical ferrate (VI) for degradation of trichloroethylene in the aqueous phase. *Desalin Water Treat* 2016; 57(11): 5138-45. <https://doi.org/10.1080/19443994.2014.1001440>
- [26] Barişçi S, Ulu F, Sillanpää M, Dimoglo A. Evaluation of flurbiprofen removal from aqueous solution by electrosynthesized ferrate (VI) ion and electrocoagulation process. *Chem Eng J* 2015; 262: 1218-25. <https://doi.org/10.1016/j.cej.2014.10.083>
- [27] Sun X, Zhang Q, Liang H, Ying L, Xiangxu M, Sharma VK. Ferrate (VI) as a greener oxidant: Electrochemical generation and treatment of phenol. *J Hazard Mater* 2015.
- [28] Zhou Z, Jiang J-Q. Treatment of selected pharmaceuticals by ferrate (VI): Performance, kinetic studies and identification of oxidation products. *J Pharm Biomed Anal* 2015; 106: 37-45. <https://doi.org/10.1016/j.jpba.2014.06.032>
- [29] Jiang J-Q, Zhou Z, Patibandla S, Shu X. Pharmaceutical removal from wastewater by ferrate (VI) and preliminary

- effluent toxicity assessments by the zebrafish embryo model. *Microchem J* 2013; 110: 239-45.
<https://doi.org/10.1016/j.microc.2013.04.002>
- [30] Manoli K, Nakhla G, Ray AK, Sharma VK. Enhanced oxidative transformation of organic contaminants by activation of ferrate (VI): Possible involvement of Fe V/Fe IV species. *Chem Eng J* 2017; 307: 513-7.
<https://doi.org/10.1016/j.cej.2016.08.109>
- [31] Tomic M, Bujanovic LN, Cekerevac M, Zdravkovic M. Application of electrochemically synthesized ferrate (VI) in the treatment of phenol contaminated wastewater from wood industry. *Acta Tech Corviniensis-Bull Eng* 2017; 10(1): 39.
- [32] Turkay O, Barışçi S, Dimoglo A. Kinetics and mechanism of methylene blue removal by electro-synthesized ferrate (VI). *Sep Sci Technol* 2016; 51(11): 1924-31.
<https://doi.org/10.1080/01496395.2016.1182189>
- [33] Myers RH, Montgomery DC, Anderson-Cook CM. *Response surface methodology: process and product optimization using designed experiments*: John Wiley & Sons 2009.
- [34] Bezerra MA, Santelli RE, Oliveira EP, Villar LS, Escalera LA. Response surface methodology (RSM) as a tool for optimization in analytical chemistry. *Talanta* 2008; 76(5): 965-77.
<https://doi.org/10.1016/j.talanta.2008.05.019>
- [35] Baş D, Boyacı İH. Modeling and optimization I: Usability of response surface methodology. *J Food Eng* 2007; 78(3): 836-45.
<https://doi.org/10.1016/j.jfoodeng.2005.11.024>
- [36] Sohail Y, Parag B, Nemeswaree B, Giorgio R. Optimizing Organophosphorus Fire Resistant Finish for Cotton Fabric Using Box-Behnken Design. *Int J Environ Res* 2016; 10(2): 313-20.
- [37] Domínguez JnR, González T, Palo P, Sánchez-Martín J. Electrochemical advanced oxidation of carbamazepine on boron-doped diamond anodes. Influence of operating variables. *Ind Eng Chem Res* 2010; 49(18): 8353-9.
- [38] Benatti CT, Tavares CRG, Guedes TA. Optimization of Fenton's oxidation of chemical laboratory wastewaters using the response surface methodology. *J Environ Manage* 2006; 80(1): 66-74.
<https://doi.org/10.1016/j.jenvman.2005.08.014>
- [39] Arslan-Alaton I, Yalabik AB, Olmez-Hanci T. Development of experimental design models to predict Photo-Fenton oxidation of a commercially important naphthalene sulfonate and its organic carbon content. *Chem Eng J* 2010; 165(2): 597-606.
<https://doi.org/10.1016/j.cej.2010.10.003>
- [40] Vepsäläinen M, Ghiasvand M, Selin J, Pienimaa J, Repo E, Pulliainen M, *et al.* Investigations of the effects of temperature and initial sample pH on natural organic matter (NOM) removal with electrocoagulation using response surface method (RSM). *Sep Purif Technol* 2009; 69(3): 255-61.
<https://doi.org/10.1016/j.seppur.2009.08.001>
- [41] Barışçi S, Ulu F, Sarkka H, Dimoglo A, Sillanpaa M. Electrosynthesis of Ferrate (VI) ion Using High Purity Iron Electrodes: Optimization of Influencing Parameters on the Process and Investigating Its Stability. *Int J Electrochem Sci* 2014; 9(6): 3099-107.

Received on 15-11-2016

Accepted on 22-02-2017

Published on 19-06-2017

DOI: <https://doi.org/10.6000/1929-5030.2017.06.02.3>